Check for updates

Monodisperse CoSn$_2$ and FeSn$_2$ nanocrystals as high-performance anode materials for lithium-ion batteries†

Shutao Wang, ‡[a,b] Meng He,‡[a,b] Marc Walter,[a,b] Frank Krumeich,[a] Kostiantyn V. Kravchyk [a,b] and Maksym V. Kovalenko ★[a,b]

Nanostructured metal alloys show great promise as replacement materials for graphite anodes, and could improve the energy and power density of present-day lithium-ion batteries (LIBs). Herein, we report a facile colloidal synthesis of CoSn$_2$ and FeSn$_2$ nanocrystals (NCs) *via* the reaction of Co or Fe NCs and SnCl$_2$ in oleylamine under reducing conditions. Among our pure Sn NCs and mixtures of Co or Fe and Sn NCs, monodisperse CoSn$_2$ nanoalloys showed considerably improved cycling stability. In particular, CoSn$_2$ delivered a stable average capacity of 650 mA h g^{-1} for 5000 cycles at a high current density of 1984 mA g^{-1}, which is among the highest reported cycling stabilities for Sn-based anode materials.

Rechargeable lithium-ion batteries (LIBs) are the main electricity storage technology for portable electronic devices and electric vehicles owing to their high energy densities, long cycling lifetimes, and high power performance.[1] Improvements to present-day LIBs might be achieved by partial or complete replacement of graphite – the major commercial anode material with a charge storage capacity of 372 mA h g^{-1} – by alloying or application of conversion-type materials with higher capacities.[2–4] Tin (Sn) is a promising candidate for replacing graphite owing to its high charge storage capacity (992 mA h g^{-1} for Li$_{22}$Sn$_5$ formation).[5–9] However, harnessing the storage ability of Sn is complicated by its poor capacity retention owing to the large volume changes (up to 300%) during lithiation/delithiation. This effect leads to mechanical disintegration of the electrodes and thus loss of electrical connectivity. These difficulties can be mitigated through nanostructuring, in particular, when the active material is embedded into an elastic and conductive network.[9–20] For example, the cycling performance of 10 nm Sn nanocrystals (NCs), syn-

thesized through colloidal methods, was demonstrated to be better than that of 150–50 nm Sn NCs.[9] As an alternative to scaling the active material, alloying with other metals (such as M–Sn alloys) has also been demonstrated to be an effective strategy; where M is electroactive (Sb,[15,21] Ge,[22] Bi,[23] Mg[24]) or inactive (Fe,[25,26] Co,[27,28–54] Ni,[55] Cu[56]) with regard to Li. The superior performance of such alloys can be attributed to the additional metal acting as a matrix, buffering volume changes and preventing electrochemical aggregation of Sn particles.[30,57,58] Herein, we attempt to tailor the electrochemical properties of Sn by combining nanostructuring, and alloying with an electrochemically non-active metal. In particular, we combine Sn with Co or Fe, which are two metals that do not form alloys with Li. On the basis of bulk phase diagrams and earlier studies on microcrystalline materials,[29,30,32,59] we targeted the synthesis of CoSn$_2$ and FeSn$_2$ NCs. We then aimed to determine whether uniform CoSn$_2$ and FeSn$_2$ nanoalloys, composed of mixed elements with atomic homogeneity, exhibit advantageous electrochemical performances compared with those of elemental Sn NCs and their mixtures with Co (Fe) NCs (obtained by simple mechanical mixing). Although there have been many studies on Co–Sn[27,28,36–38,41,45] and Fe–Sn[25,26] nanoscopic alloys for LIBs, our comparative study requires Co, Fe, Sn, CoSn$_2$, and FeSn$_2$ to be obtained in the form of uniform colloidal NCs of very similar sizes. After accomplishing these syntheses, we find that both CoSn$_2$ and FeSn$_2$ NCs are indeed unlike the mixtures of their elemental NCs. Higher capacities and extended cyclabilities were achieved, highlighting the importance of the nanoscopic homogeneity of alloyed NCs.

CoSn$_2$ NCs were synthesized *via* successive reduction of Co and Sn precursors. First, dried oleylamine was mixed with CoCl$_2$, and further dried under vacuum followed by injection of a LiN(iPr)$_2$ (lithium diisopropylamide, LDA) solution at 270 °C, and, 30 s later at 235 °C, injection of SnCl$_2$ into the solution. In this reaction, the LDA served as a mild base for the partial deprotonation of oleylamine, thereby promoting the formation of highly reactive metal-oleylamido complexes.[9,60] The latter species almost instantly decomposed, causing a burst of nucleation and NC formation. The reaction

[a]ETH Zürich, Department of Chemistry and Applied Biosciences, Vladimir Prelog Weg 1, 8093 Zürich, Switzerland
[b]Empa-Swiss Federal Laboratories for Materials Science and Technology, Laboratory for thin films and photovoltaics, Überlandstrasse 129, 8600 Dübendorf, Switzerland. E-mail: mvkovalenko@ethz.ch
†Electronic supplementary information (ESI) available. See DOI: 10.1039/c7nr08261d
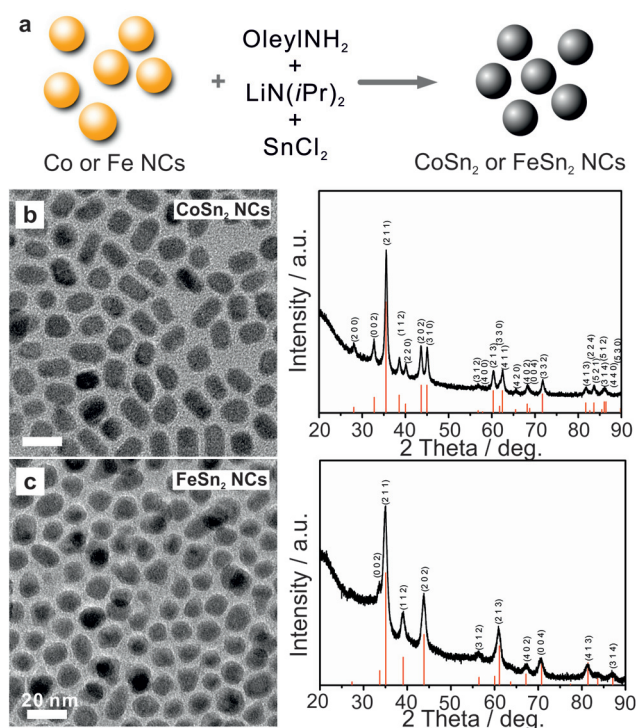‡These authors contributed equally.

Fig. 1 (a) Schematic illustration of one-pot synthesis, TEM and corresponding XRD patterns of (b) CoSn₂ and (c) FeSn₂ NCs.

mixture was maintained at *ca.* 235 °C for an additional 4 h to form uniform Co–Sn alloy NCs.

Transmission electron microscopy (TEM) images and X-ray diffraction (XRD) patterns (Fig. 1b) confirmed the formation of uniform and highly crystalline tetragonal $CoSn_2$ NCs (space group $I4/mcm$, $a = b = 6.363$ Å, $c = 5.456$ Å, JCPDS no. 25-0256) with sizes on the order of 10 nm. Crystalline $FeSn_2$ NCs (JCPDS no. 25-0415, space group $I4/mcm$, $a = b = 6.539$ Å, $c = 5.325$ Å) of the same average size could be synthesized in a similar fashion by replacing $CoCl_2$ with $FeCl_2$ (Fig. 1c, for experimental details see ESI†). Notably, the size of the $CoSn_2$ NCs could be tuned in the range of 5–13 nm with a narrow size-dispersion (Table S1, Fig. S1†). To compare the characteristics of the alloys and pure metals, we also synthesized elemental Sn and Co NCs, using previously published procedures (see examples on Fig. S2†).[9,60] The galvanostatic cycling measurements for $CoSn_2$ NCs are summarized in Fig. 2. The as-synthesized NCs were surface-functionalized with long-chain capping molecules (namely, oleylamine and oleic acid), rendering the NCs colloidally stable in non-polar solvents. For electrochemical testing, these electrically insulating molecular layers were removed by treatment with a 1 M solution of hydrazine in acetonitrile (ACN) for 2 h, a treatment typically used for colloidal quantum dots.[61] Untreated NCs yielded no operational electrodes.

All electrodes contained 64 wt% of active material, 15 wt% carboxymethylcellulose (CMC) as binder and 21 wt% carbon black as a conductive additive. Electrochemical tests were performed in Li-ion half-cells with elemental lithium acting as both counter and reference electrode.
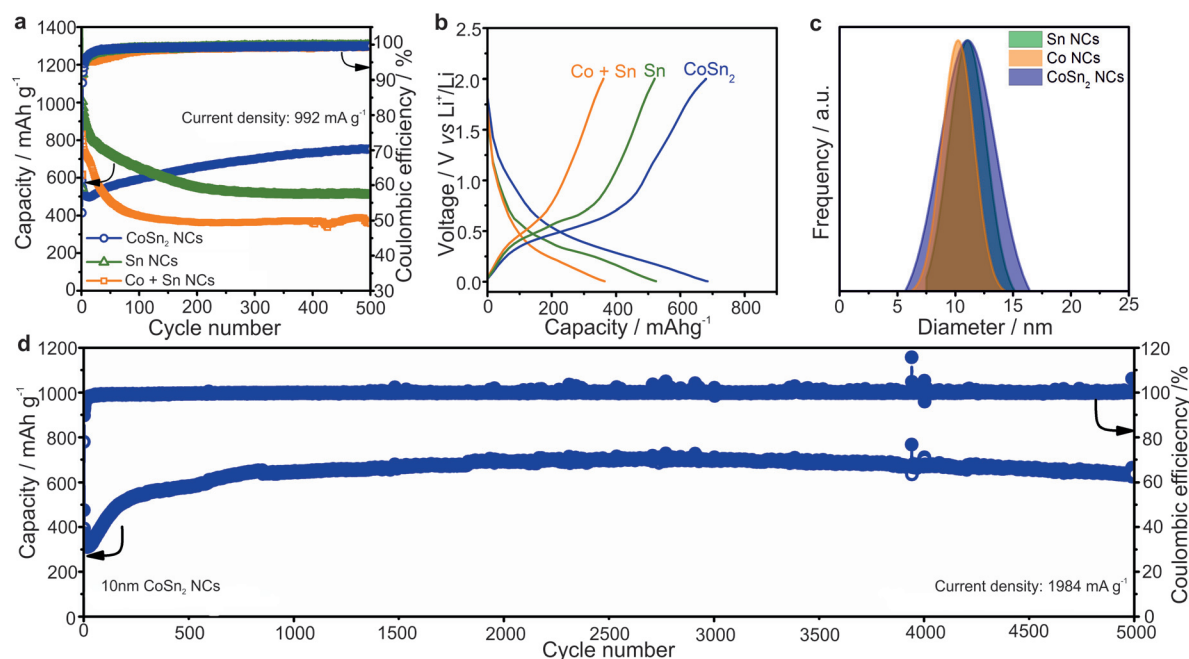

Fig. 2 (a) Comparison of the cycling stability for CoSn₂ NCs, Sn NCs and mixtures of Co NCs with two equivalents of Sn NCs, all of *ca.* 10–12 nm mean particle size, in Li-ion half-cells at a current density of 992 mA g⁻¹. Initial coulombic efficiencies of CoSn₂ NCs, Sn NCs and mixture of Co and Sn NCs were 52%, 59% and 63%. (b) Corresponding galvanostatic charge/discharge curves for the 250th cycle. (c) Size distributions of the tested NCs (obtained with Nano Measurer software). (d) Long-term cycling stability of *ca.* 10 nm CoSn₂ NCs at current density of 1984 mA g⁻¹. All cells were cycled at room temperature in the potential range of 0.005–2.000 V *vs.* Li⁺/Li.

A comparison of the capacity retention of CoSn$_2$, Sn, and mixtures of Co NCs with two equivalents of Sn NCs for cycling at a current density of 992 mA g^{-1} (rate of 1C for Sn) is shown in Fig. 2a (all NCs were *ca.* 10 nm large).

In agreement with the higher theoretical capacity of Sn (992 mA h g^{-1} *vs.* 795 mA h g^{-1} for CoSn$_2$), the Sn NCs delivered the highest capacities in the first cycles. However, upon prolonged cycling, the capacity of the Sn NCs, and mechanical mixtures of Sn and Co NCs, gradually decreased. Conversely, the capacities of the CoSn$_2$ NCs increased to ~750 mA h g^{-1}. In all cases, the coulombic efficiency was initially low, but increased to more than 99%. However, the most distinct feature of the CoSn$_2$ NCs was their high long-term cycling stability, even at high cycling rates (see Fig. 2d). In particular, at a current density of 1984 mA g^{-1}, very stable capacities, on average 650 mA h g^{-1}, were obtained up to 5000 cycles.

As follows from *ex situ* XRD measurements of CoSn$_2$ NCs before and after electrochemical cycling (Fig. 3), CoSn$_2$ phase can be fully recovered after delithiation reaction suggesting that the overall lithiation and delithiation mechanism of CoSn$_2$ NCs can be described by the equation:

$$CoSn_2 + 8.8\, Li^+ + 8.8e^- \leftrightarrow 2Li_{4.4}Sn + Co. \qquad (1)$$

Ex situ XRD measurements of the CoSn$_2$ NC electrodes show continuous amorphization of the material during cycling as indicated by the steady decrease of the signal intensity and broadening of the peaks. The anisotropic expansion of such amorphous phases can lead to lower mechanical stress during cycling, compared with that of crystalline elemental Sn NCs, which may explain the observed high cycling stability of CoSn$_2$ NCs. In addition, the amorphization of CoSn$_2$ NCs during cycling might facilitate the lithation/delithiation reaction and therefore lead to a higher utilization of the capacity as indicated by the increasing values during initial cycling. Notably, the *ex situ* XRD measurements indicate that Co-domains are not fully inactive after the first lithiation, but take a part in full CoSn$_2$ recovery.

Similar electrochemical cycling behavior was obtained with FeSn$_2$ NCs (Fig. 4). Namely, stable capacities in the range of
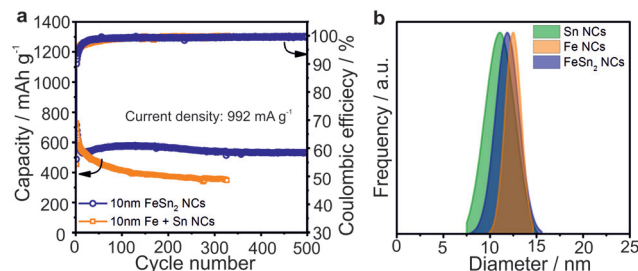

Fig. 4 (a) Comparison of the cycling stability for FeSn$_2$ NCs and mixtures of Sn and Fe NCs in Li-ion half-cells at a current density of 992 mA g^{-1} (see Fig. S4 and S5† for comparison of cycling stability and rate capability of FeSn$_2$ and CoSn$_2$ NCs) with (b) the corresponding size distributions (obtained with Nano Measurer software) of all tested NCs. Initial coulombic efficiencies of FeSn$_2$ NCs and mixture of Fe and Sn NCs were 56% and 54%. All cells were cycled at room temperature in the potential range 0.005–2.0 V *vs.* Li$^+$/Li with sodium alginate as binder.

500–600 mA h g^{-1} were retained for at least 500 cycles, clearly outperforming mixtures of Sn and Fe NCs of a similar size. We attribute this effect to the closer contact of Fe and Sn domains due to the full recovery of FeSn$_2$ phase after charge (see Fig. S3†), which can lead to a more effective buffering of the volume changes and prevent aggregation of Sn-domains.

Conclusions

In conclusion, we have developed a novel synthesis of highly uniform colloidal CoSn$_2$ and FeSn$_2$ NCs, all with mean particle sizes in the range of 10–12 nm. Both CoSn$_2$ and FeSn$_2$ NCs showed electrochemical performance superior to that of Sn NCs and mixtures of individual Sn and Co or Fe NCs. In particular, CoSn$_2$ NCs exhibited high reversible specific charge-storage capacities and cycling stability. Specifically, CoSn$_2$ NCs delivered a stable average capacity of 650 mA h g^{-1} for 5000 cycles at a high density of 1984 mA g^{-1} (rate of 2C for Sn). This high-performance cycling stability can be attributed to the presence of Co domains, which acted as a matrix that buffers the volumetric changes occurring during lithiation/delithiation, and prevents the aggregation of Sn NCs and amorphization of the electrode material. Such high-rate performance illustrates the potential for use of nanostructured Co–Sn materials, or their mixtures with graphite, as alternative anode materials for high-power Li-ion batteries.

Conflicts of interest

There are no conflicts to declare.

Acknowledgements
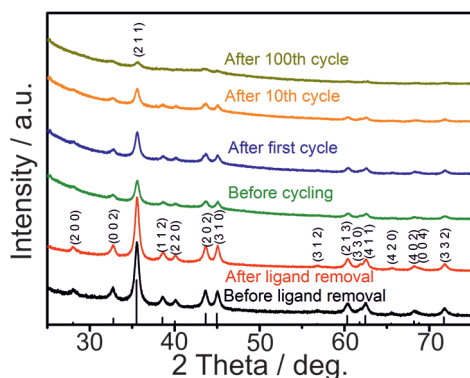
Fig. 3 *Ex situ* XRD patterns of CoSn$_2$ NCs before and after (charged CoSn$_2$ NCs) electrochemical cycling.

Notes and references

1 M. Armand and J. M. Tarascon, *Nature*, 2008, **451**, 652–657.

2 Y. Yao, N. Xu, D. Guan, J. Li, Z. Zhuang, L. Zhou, C. Shi, X. Liu and L. Mai, *ACS Appl. Mater. Interfaces*, 2017, **9**, 39425–39431.

3 C. Tang, Y. Liu, C. Xu, J. Zhu, X. Wei, L. Zhou, L. He, W. Yang and L. Mai, *Adv. Funct. Mater.*, 2018, **28**, 1704561.

4 C. Tang, J. Zhu, X. Wei, L. He, K. Zhao, C. Xu, L. Zhou, B. Wang, J. Sheng and L. Mai, *Energy Storage Mater.*, 2017, **7**, 152–156.

5 W. M. Zhang, J. S. Hu, Y. G. Guo, S. F. Zheng, L. S. Zhong, W. G. Song and L. J. Wan, *Adv. Mater.*, 2008, **20**, 1160–1165.

6 G. Derrien, J. Hassoun, S. Panero and B. Scrosati, *Adv. Mater.*, 2007, **19**, 2336–2340.

7 M. Wachtler, J. O. Besenhard and M. Winter, *J. Power Sources*, 2001, **94**, 189–193.

8 Y. Xu, Q. Liu, Y. Zhu, Y. Liu, A. Langrock, M. R. Zachariah and C. Wang, *Nano Lett.*, 2013, **13**, 470–474.

9 K. Kravchyk, L. Protesescu, M. I. Bodnarchuk, F. Krumeich, M. Yarema, M. Walter, C. Guntlin and M. V. Kovalenko, *J. Am. Chem. Soc.*, 2013, **135**, 4199–4202.

10 P. G. Bruce, B. Scrosati and J.-M. Tarascon, *Angew. Chem., Int. Ed.*, 2008, **47**, 2930–2946.

11 M. R. Palacin, *Chem. Soc. Rev.*, 2009, **38**, 2565–2575.

12 A. Magasinski, P. Dixon, B. Hertzberg, A. Kvit, J. Ayala and G. Yushin, *Nat. Mater.*, 2010, **9**, 353–358.

13 C. K. Chan, R. N. Patel, M. J. O'Connell, B. A. Korgel and Y. Cui, *ACS Nano*, 2010, **4**, 1443–1450.

14 M. F. Oszajca, M. I. Bodnarchuk and M. V. Kovalenko, *Chem. Mater.*, 2014, **26**, 5422–5432.

15 M. He, M. Walter, K. V. Kravchyk, R. Erni, R. Widmer and M. V. Kovalenko, *Nanoscale*, 2015, **7**, 455–459.

16 M. He, K. Kravchyk, M. Walter and M. V. Kovalenko, *Nano Lett.*, 2014, **14**, 1255–1262.

17 J. B. Cook, E. Detsi, Y. Liu, Y.-L. Liang, H.-S. Kim, X. Petrissans, B. Dunn and S. H. Tolbert, *ACS Appl. Mater. Interfaces*, 2017, **9**, 293–303.

18 Y. Jin, Y. Tan, X. Hu, B. Zhu, Q. Zheng, Z. Zhang, G. Zhu, Q. Yu, Z. Jin and J. Zhu, *ACS Appl. Mater. Interfaces*, 2017, **9**, 15388–15393.

19 H. Zhang, X. Huang, O. Noonan, L. Zhou and C. Yu, *Adv. Funct. Mater.*, 2017, **27**, 1606023.

20 M. Walter, M. I. Bodnarchuk, K. V. Kravchyk and M. V. Kovalenko, *Chimia*, 2015, **69**, 724–728.

21 M. Walter, S. Doswald and M. V. Kovalenko, *J. Mater. Chem. A*, 2016, **4**, 7053–7059.

22 M. I. Bodnarchuk, K. V. Kravchyk, F. Krumeich, S. Wang and M. V. Kovalenko, *ACS Nano*, 2014, **8**, 2360–2368.

23 A. Trifonova, M. Wachtler, M. Winter and J. O. Besenhard, *Ionics*, 2002, **8**, 321–328.

24 D. Larcher, A. S. Prakash, J. Saint, M. Morcrette and J. M. Tarascon, *Chem. Mater.*, 2004, **16**, 5502–5511.

25 Y. Ye, P. Wu, X. Zhang, T. G. Zhou, Y. W. Tang, Y. M. Zhou and T. H. Lu, *RSC Adv.*, 2014, **4**, 17401–17404.

26 C. Q. Zhang, J. P. Tu, X. H. Huang, Y. F. Yuan, S. F. Wang and F. Mao, *J. Alloys Compd.*, 2008, **457**, 81–85.

27 X. Y. Fan, F. S. Ke, G. Z. Wei, L. Huang and S. G. Sun, *J. Alloys Compd.*, 2009, **476**, 70–73.

28 B. Feng, J. Xie, G. S. Cao, T. J. Zhu and X. B. Zhao, *New J. Chem.*, 2013, **37**, 474–480.

29 A. D. W. Todd, R. E. Mar and J. R. Dahn, *J. Electrochem. Soc.*, 2007, **154**, A597–A604.

30 S.-I. Lee, S. Yoon, C.-M. Park, J.-M. Lee, H. Kim, D. Im, S.-G. Doo and H.-J. Sohn, *Electrochim. Acta*, 2008, **54**, 364–369.

31 P. P. Ferguson, A. D. W. Todd and J. R. Dahn, *Electrochem. Commun.*, 2008, **10**, 25–31.

32 P. P. Ferguson, M. L. Martine, A. E. George and J. R. Dahn, *J. Power Sources*, 2009, **194**, 794–800.

33 Z. Chen, J. Qian, X. Ai, Y. Cao and H. Yang, *J. Power Sources*, 2009, **189**, 730–732.

34 X.-Y. Fan, F.-S. Ke, G.-Z. Wei, L. Huang and S.-G. Sun, *J. Alloys Compd.*, 2009, **476**, 70–73.

35 L. Huang, J.-S. Cai, Y. He, F.-S. Ke and S.-G. Sun, *Electrochem. Commun.*, 2009, **11**, 950–953.

36 F. Nacimiento, R. Alcántara and J. L. Tirado, *J. Electrochem. Soc.*, 2010, **157**, A666–A671.

37 J. He, H. Zhao, J. Wang, J. Wang and J. Chen, *J. Alloys Compd.*, 2010, **508**, 629–635.

38 X.-L. Wang, W.-Q. Han, J. Chen and J. Graetz, *ACS Appl. Mater. Interfaces*, 2010, **2**, 1548–1551.

39 F. Nacimiento, P. Lavela, J. Tirado and J. Jiménez-Mateos, *J. Solid State Electrochem.*, 2012, **16**, 953–962.

40 G. Ferrara, L. Damen, C. Arbizzani, R. Inguanta, S. Piazza, C. Sunseri and M. Mastragostino, *J. Power Sources*, 2011, **196**, 1469–1473.

41 Z. Du and S. Zhang, *J. Phys. Chem. C*, 2011, **115**, 23603–23609.

42 L.-J. Xue, Y.-F. Xu, L. Huang, F.-S. Ke, Y. He, Y.-X. Wang, G.-Z. Wei, J.-T. Li and S.-G. Sun, *Electrochim. Acta*, 2011, **56**, 5979–5987.

43 M.-Y. Li, C.-L. Liu, M.-R. Shi and W.-S. Dong, *Electrochim. Acta*, 2011, **56**, 3023–3028.

44 D.-H. Nam, R.-H. Kim, C.-L. Lee and H.-S. Kwon, *J. Electrochem. Soc.*, 2012, **159**, A1822–A1826.

45 G. Ferrara, C. Arbizzani, L. Damen, M. Guidotti, M. Lazzari, F. G. Vergottini, R. Inguanta, S. Piazza, C. Sunseri and M. Mastragostino, *J. Power Sources*, 2012, **211**, 103–107.

46 R. M. Gnanamuthu, Y. N. Jo and C. W. Lee, *J. Alloys Compd.*, 2013, **564**, 95–99.

47 J. R. Gonzalez, F. Nacimiento, R. Alcantara, G. F. Ortiz and J. L. Tirado, *CrystEngComm*, 2013, **15**, 9196–9202.

48 X. Liu, J. Xie, H. Zhao, P. Lv, K. Wang, Z. Feng and K. Świerczek, *Solid State Ionics*, 2015, **269**, 86–92.

49 B.-O. Jang, S.-H. Park and W.-J. Lee, *J. Alloys Compd.*, 2013, **574**, 325–330.

50 N. Mahmood, C. Zhang, F. Liu, J. Zhu and Y. Hou, *ACS Nano*, 2013, **7**, 10307–10318.

51 N. Mahmood, J. Zhu, S. Rehman, Q. Li and Y. Hou, *Nano Lett.*, 2015, **15**, 755–765.

52 G. O. Park, J. Yoon, J. K. Shon, Y. S. Choi, J. G. Won, S. B. Park, K. H. Kim, H. Kim, W.-S. Yoon and J. M. Kim, *Adv. Funct. Mater.*, 2016, **26**, 2800–2808.

53 X. Shi, H. Song, A. Li, X. Chen, J. Zhou and Z. Ma, *J. Mater. Chem. A*, 2017, **5**, 5873–5879.

54 J. Zhu, D. Wang, T. Liu and C. Guo, *Electrochim. Acta*, 2014, **125**, 347–353.

55 J. Liu, Y. R. Wen, P. A. van Aken, J. Maier and Y. Yu, *Nano Lett.*, 2014, **14**, 6387–6392.

56 W. X. Lei, Y. Pan, Y. C. Zhou, W. Zhou, M. L. Peng and Z. S. Ma, *RSC Adv.*, 2014, **4**, 3233–3237.

57 N. Tamura, Y. Kato, A. Mikami, M. Kamino, S. Matsuta and S. Fujitani, *J. Electrochem. Soc.*, 2006, **153**, A1626–A1632.

58 C. M. Ionica-Bousquet, P. E. Lippens, L. Aldon, J. Olivier-Fourcade and J. C. Jumas, *Chem. Mater.*, 2006, **18**, 6442–6447.

59 L. O. Vogt and C. Villevieille, *J. Mater. Chem. A*, 2017, **5**, 3865–3874.

60 M. He, L. Protesescu, R. Caputo, F. Krumeich and M. V. Kovalenko, *Chem. Mater.*, 2015, **27**, 635–647.

61 D. V. Talapin and C. B. Murray, *Science*, 2005, **310**, 86–89.